

# Influence of External Electric Field on the Primary Mechanisms of Kerogen

Yanlong Guan, Xiaowei Zhang, and Yudou Wang \*

School of Science, China University of Petroleum (East China), Qingdao, 266580, China

**Abstract.** The pyrolysis of kerogen, a critical step in hydrocarbon generation from oil shale, is profoundly affected by external stimuli, particularly thermal conditions and applied electric fields. The complex molecular structure of kerogen, mainly composed of carbon, hydrogen, oxygen, nitrogen, and sulfur, leads to distinct pyrolysis behaviors under various conditions. This study explores the effects of an alternating electric field (AC field) on kerogen pyrolysis, particularly focusing on the frequency-dependent promotion of reaction kinetics and product distribution. Molecular dynamics (MD) simulations, utilizing the reactive force field (ReaxFF) and the QTPIE (charge transfer with polarization current equilibration) method, reveal that electric fields, especially at frequencies of 150 GHz, can accelerate kerogen decomposition. The study identifies a critical temperature of 1250 K as the threshold for significant molecular breakdown and demonstrates that external electric fields promote pyrolysis by optimizing molecular energy transfer, particularly at 150 GHz. This has implications for improving the efficiency and selectivity of shale oil and gas production.

**Keywords:** Kerogen pyrolysis; ReaxFF; Alternating electric field; QTPIE.

## 1. Introduction

Kerogen is a complex macromolecular organic substance and serves as a crucial precursor for the formation of petroleum and natural gas. It is widely distributed in oil shale, coal, and other sedimentary rocks [1,2]. As the most abundant form of solid organic carbon on Earth, the pyrolysis of kerogen plays a pivotal role in the formation and conversion of fossil fuel [3]. In particular, in the development of unconventional energy resources, the pyrolysis efficiency of kerogen directly affects the yield and quality of shale oil and shale gas [4]. Kerogen possesses a highly cross-linked and intricate molecular structure, primarily composed of carbon, hydrogen, oxygen, nitrogen, and sulfur. The chemical composition and structure of kerogen vary significantly depending on its origin and geological region [5,6]. These inherent characteristics result in distinct reaction pathways and kinetic behaviors during the pyrolysis process, which are strongly influenced by factors such as temperature, pressure, and the chemical environment [7]. In recent years, optimizing the kerogen pyrolysis process to enhance the utilization efficiency of unconventional energy has become a research focus [8-11].

The thermal decomposition of kerogen, the predominant organic component in oil shale, plays a pivotal role in hydrocarbon generation and energy extraction [12]. Understanding the factors influencing kerogen pyrolysis is critical for optimizing resource utilization and enhancing energy conversion efficiency. Previous studies have extensively explored the effects of minerals, temperature, and catalytic agents on kerogen degradation. For instance, MD simulations revealed that montmorillonite, a common clay mineral in oil shale, significantly accelerates kerogen pyrolysis by altering molecular interactions and reducing activation energies [13]. Additionally, experimental studies demonstrated that minerals like gypsum exhibit catalytic effects, while carbonates may inhibit hydrocarbon generation, highlighting the complexity of inorganic-organic interactions during pyrolysis [14].

Despite these advancements, the role of external physical fields, particularly electric fields, in modulating kerogen pyrolysis remains underexplored [15]. External electric fields have been shown to influence chemical reactions by polarizing molecular structures, altering reaction pathways, and reducing energy barriers in various systems, such as polymer decomposition and catalytic processes. However, their application in kerogen thermal degradation has been rarely reported. This

knowledge gap limits the development of innovative techniques for enhancing hydrocarbon yield or controlling product distribution under non-thermal stimuli [16].

To address this issue, the current investigation utilizes MD computational approaches to comprehensively examine the influence of applied electric fields on thermal decomposition processes in kerogen systems. Drawing on methodologies from prior MD studies on montmorillonite-kerogen systems [13], we aim to quantify field-induced changes in pyrolysis kinetics, product distributions, and molecular-scale mechanisms. The findings will provide theoretical insights into the interplay between electric fields and kerogen's structure evolution, potentially offering new strategies for energy-efficient shale oil recovery or in-situ conversion technologies. By integrating thermal and electric field effects, this work advances the fundamental understanding of kerogen pyrolysis dynamics and contributes to the broader goal of sustainable energy resource development.

## 2. Theoretical approach

### 2.1 ReaxFF-MD approach

ReaxFF is a reactive MD method that differs fundamentally from traditional classical force fields. Unlike conventional approaches, ReaxFF not only describes static intermolecular interactions but also explicitly models bond formation and rupture, making it particularly suitable for simulating complex reactive systems such as combustion, catalytic pyrolysis, and other chemically dynamic processes.

The core of ReaxFF lies in its incorporation of atomic bond-level information through parameterized relationships for bond length-energy, angular potentials, and non-bonded interactions. These relationships collectively determine molecular structures and reactive potential energy surfaces. The ability of ReaxFF to effectively describe chemical reactions stems from its reliance on bond-order theory, originally proposed by Abell and Tersoff. This theory quantifies the strength of chemical bonds between atoms and is dynamically integrated into ReaxFF to adjust interatomic interactions during bond breaking. The mathematical representation of bond order (BO<sub>ij</sub>) is formulated in Eq. (1) as demonstrated below [17]:

$$BO'_{ij} = BO'_{ij}{}^{\sigma} + BO'_{ij}{}^{\pi} + BO'_{ij}{}^{\pi\pi} = \exp \left[ p_{bo1} \left( \frac{r_{ij}}{r_0^{\sigma}} \right)^{p_{bo2}} \right] + \exp \left[ p_{bo3} \left( \frac{r_{ij}}{r_0^{\pi}} \right)^{p_{bo4}} \right] + \exp \left[ p_{bo5} \left( \frac{r_{ij}}{r_0^{\pi\pi}} \right)^{p_{bo6}} \right] \quad (1)$$

where  $BO'_{ij}$ ,  $BO'_{ij}{}^{\sigma}$ ,  $BO'_{ij}{}^{\pi}$ ,  $BO'_{ij}{}^{\pi\pi}$ ,  $r_0^{\sigma}$ ,  $r_0^{\pi}$ ,  $r_0^{\pi\pi}$ ,  $p_{bo1}$ – $p_{bo6}$  correspond to the origin bond order, bond terms for single bond, bond terms for double bond, bond terms for triple bond, equilibrium distance of single bond, equilibrium distance of double bond, equilibrium distance of triple bond, different ReaxFF regression empirical parameters.

The total energy of the system in ReaxFF is expressed as a summation of multiple energy terms, which bridging classical force field interactions with quantum mechanical reaction dynamics:

$$E_{\text{system}} = E_{\text{bond}} + E_{\text{over}} + E_{\text{under}} + E_{\text{val}} + E_{\text{pen}} + E_{\text{tors}} + E_{\text{conj}} + E_{\text{vdWaals}} + E_{\text{Coulomb}} \quad (2)$$

where  $E_{\text{bond}}$ ,  $E_{\text{over}}$ ,  $E_{\text{under}}$ ,  $E_{\text{val}}$ ,  $E_{\text{pen}}$ ,  $E_{\text{tors}}$ ,  $E_{\text{conj}}$ ,  $E_{\text{vdWaals}}$ , and  $E_{\text{Coulomb}}$  correspond to the bond energy, overcoordination atomic energies, undercoordination atomic energies, valence angle energy, penalty energy, torsion energy, conjugation effects, van der Waals mutual effects, and Coulomb mutual effects, respectively.

### 2.2 Modeling of External Electric Fields

The application of an external electric field induces charge redistribution within molecular systems by displacing electron density relative to nuclear positions, thereby generating field-dependent dipole moments. Consequently, rigorous modeling of such electrostatic interactions requires computational approaches that explicitly account for electronic polarization effects through the incorporation of molecular polarizability parameters in the potential energy functions.

Precise characterization of electronic charge redistribution and dipole moment variations represents a fundamental requirement for reliable MD investigations of electric field induced kerogen decomposition processes. The charge distribution was computed using the Charge Transfer with Polarization by Ionic Equilibration method [18,19], a polarizable charge equilibration approach that explicitly incorporate both charge transfer and electronic polarization effects. The QTPIE method defines atomic charges by minimizing the total electrostatic energy of the system under the constraint of charge conservation. The energy functional is expressed as:

$$E_{\text{QTPIE}} = \sum_i (\chi_i q_i + \frac{1}{2} J_{ii} q_i^2) + \sum_{i \neq j} \frac{1}{2} J_{ij} q_i q_j + \sum_i \frac{1}{2} \alpha_i (p_i \cdot p_i) \quad (3)$$

where  $\chi_i$  is the electronegativity,  $J_{ij}$  represents the Coulomb interaction between atoms  $i$  and  $j$ ,  $q_i$  is the atomic charge,  $\alpha_i$  is the atomic polarizability, and  $p_i$  denotes the induced dipole moment. The inclusion of the polarization term ( $p_i$ ) distinguishes QTPIE from traditional charge equilibration (QEq) methods [19,20], which neglect explicit polarization and rely solely on charge transfer to minimize electronegativity differences.

The QEq method defines the energy functional as:

$$E_{\text{QEq}} = \sum_i (\chi_i q_i + \frac{1}{2} J_{ii} q_i^2) + \sum_{i \neq j} \frac{1}{2} J_{ij} q_i q_j \quad (4)$$

which lacks the polarization term  $\sum_i \frac{1}{2} \alpha_i (p_i \cdot p_i)$ . This difference is crucial in distinguishing the two approaches. The polarization term in QTPIE accounts for the induced dipoles and allows for dynamic adjustments of the electron cloud under external electric fields, which is essential for simulating real physical phenomena under field perturbations.

Compared to QEq, the QTPIE framework offers two key advantages. First, its explicit polarization term allows for dynamic redistribution of electron density under external electric fields, capturing the nonlinear response of molecular dipoles to field perturbations [18]. In contrast, QEq assumes static charge distributions, leading to underestimation of polarization effects in high-field regimes. Second, QTPIE employs a dual self-consistent procedure: it iteratively solves for charges and dipoles while enforcing charge conservation, whereas QEq solves only for charges with fixed atomic hardness parameters. This dual optimization ensures a physically consistent representation of both short-range charge transfer and long-range polarization, which is essential for simulating field-induced bond breaking and radical formation in kerogen pyrolysis.

### 2.3 Simulation details

The MD simulations investigating electric field effects on kerogen pyrolysis were performed through the following computational procedures. The initial LongKou kerogen molecule model was constructed using Material Studio software [21], and the five kerogen models were geometrically optimized using the Dreiding force field in the Forcite module. To prevent atomic overlap, the initial system density was carefully set to 0.3g/cm<sup>3</sup>, generating three-dimensional configurations as illustrated in Figure 1.

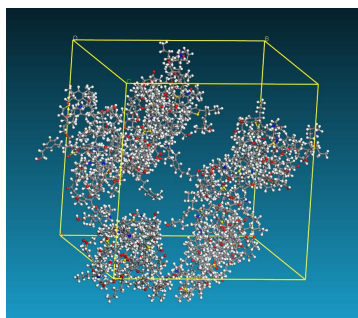


Figure. 1 Diagram of the molecular model of 3D kerogen.

Reactive MD simulations were implemented with the specialized ReaxFF force field developed by Wood et al. [22], which incorporates full valence descriptions for C/H/O/N/S elements. The

simulation parameters included a time step of 0.1 fs and cutoff radius of 0.3 Å under NVT ensemble conditions. Prior to production runs, the system underwent thermal annealing from 300 K to 600 K followed by gradual cooling to 300 K to achieve realistic kerogen configurations. Energy minimization was accomplished through conjugate gradient algorithms, with temperature regulation maintained by the Nose-Hoover thermostat using a 100 fs damping constant. System equilibration involved two critical stages: First, a 20 ps NPT-MD compression at 500 MPa elevated the density to 0.94 g/cm<sup>3</sup>, matching experimental measurements. Subsequently, a 100 ps NVT relaxation at 300 K ensured structural stability. Post-simulation analysis utilized custom Python scripts combined with OVITO visualization package for trajectory processing and statistical evaluation of reactive events.

### 3. Results and Discussion

#### 3.1 Increasing Temperature Pyrolysis

To determine the temperature for the current simulation, the kerogen system was heated from 300 K to 3500 K with a heating rate of 12.8 k/ps, and the change in the number of molecules in the system during the heating process was observed. The results are shown in Figure 2. From the graph, it is evident that as the temperature increases, there is a sharp rise in the number of molecules, particularly after reaching a temperature of approximately 1250 K. At temperatures below 1250 K, the increase in molecular production is gradual, indicating a relatively slow and less significant pyrolytic breakdown of the kerogen. However, once the temperature surpasses 1250 K, the molecular count rises sharply, indicating the onset of more intense molecular breakdown and the beginning of primary decomposition. This point can be identified as the critical threshold for initial pyrolysis of kerogen. Given this observation, the initial decomposition temperature of kerogen can be identified as approximately 1250 K. This temperature serves as a key parameter for setting the conditions in subsequent simulations. For this study, we have chosen 1250 K as the temperature at which to conduct isothermal pyrolysis simulations. The goal of these simulation is to explore the influence of an external electric field on the initial pyrolysis behavior of kerogen at this critical temperature. The simulation conducted at this temperature will provide valuable insights into the influence of the external electric field on the initial pyrolysis process.

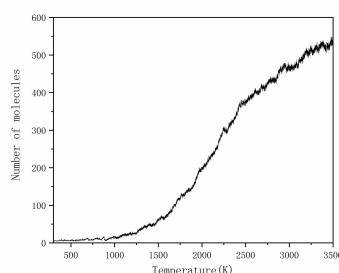


Figure. 2 Time evolution of total number of molecules during ReaxFF MD at heating rate of 12.8k/ps.

#### 3.2 Isothermal Pyrolysis

Isothermal pyrolysis of the kerogen system was conducted at 1250 K under AC fields with varying frequencies, with each simulation lasting 250 ps. Temporal variations in weight percentages of pyrolysis products—gaseous compounds, light oil, heavy oil, and coke—are illustrated in Figure 3. As depicted in Figure 3d, the AC field universally enhances kerogen pyrolysis, with the 150 GHz frequency exhibiting the most pronounced catalytic effect, followed by 200 GHz and 250 GHz. Notably, the 150 GHz field correlated with a reduced coke formation rate, as evidenced by its lower incremental curve slope compared to other frequencies, suggesting its dual role in promoting hydrocarbon generation while suppressing undesired solid residue formation. In Figure 3c, all frequencies induced steady increases in product yields, yet the 150 GHz field achieved the highest

heavy oil yield, indicating enhanced decomposition of organic matter into heavier hydrocarbons under this frequency. Figure 3a demonstrates progressive gas production during pyrolysis, with marked acceleration at 100 GHz, 150 GHz, and 250 GHz. Light oil yields (Figure 3b) followed a similar ascending trend, though growth rates plateaued after 110 ps. The maximum light oil production occurred at 200 GHz, with 150 GHz ranking second. Integrated analysis of all components reveals that the 150 GHz field optimally balances reaction dynamics. This frequency significantly accelerated the generation of gaseous species, light oil, and heavy oil while minimizing coke deposition. These findings suggest that 150 GHz may serve as a favorable frequency for enhancing pyrolysis efficiency and product selectivity. However, the identification of an absolute optimal frequency requires further investigation to account for potential influencing factors such as molecular conformation, and reaction kinetics.

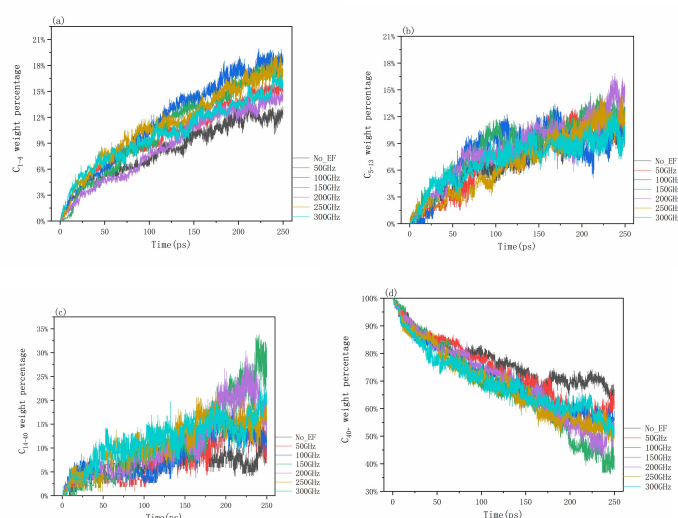


Figure. 3 Variation of weight percentage of each component at different electric field frequencies (electric field intensity is fixed at  $2\text{V}/\text{\AA}$ ) a (gas), b (light oil), c (heavy oil), d (coke).

### 3.3 Effect of AC field on carbon-oxygen (C-O) bonds

An external electric field can influence the dipole moment of molecules. Given the polarity of the C–O bond, the application of an external electric field alters the internal charge distribution of the molecule, enhancing dipole interactions and making the bond less stable and more prone to cleavage. The variation in the number of C–O bonds over time is statistically analyzed, as depicted in Figure 4. Under the condition of no electric field, the number of C–O bond breakages is the lowest, indicating that an alternating electric field overall promotes C–O bond cleavage. At frequencies of 200 GHz and 300 GHz, the C–O bond breakage rate increases compared to the no-field condition but remains relatively slow, suggesting a limited enhancement effect. At 150 GHz, the decline occurs at the fastest rate, and the number of broken C–O bonds is the highest, indicating that the 150 GHz field exhibits the strongest promotion effect on C–O bond cleavage. This effect may be attributed to a resonance mechanism that optimizes energy transfer efficiency, thereby minimizing the C–O bond dissociation energy barrier. At 50 GHz and 100 GHz, the initial bond breakage trend is relatively fast, but after 125 ps, the cleavage rate decreases, suggesting that these frequencies provide a strong initial promotion effect but exhibit an overall moderate enhancement. At 250 GHz, the bond breakage trend remains fast and is close to that at 150 GHz; however, the final number of remaining C–O bonds is slightly higher. This result suggests that high-frequency fields may induce energy overload or non-resonant effects, leading to a slightly reduced enhancement effect.

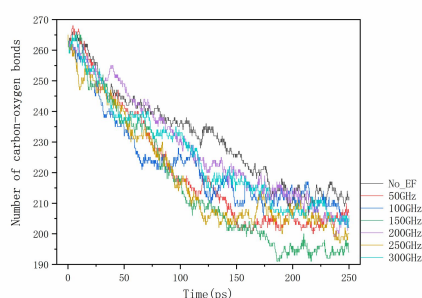


Figure. 4 Distribution of carbon-oxygen bonds over time under the action of different electric field frequencies.

### 3.4 Effect of AC field on the potential energy of kerogen pyrolysis process

The potential energy variation of the system was calculated, as shown in Figure 5. From the changes in the potential energy curves, it is evident that the trends of potential energy variation in the kerogen pyrolysis system differ significantly under different electric field frequencies. In the absence of an electric field, the potential energy of the system remains relatively stable with minor fluctuations, hovering around -49300 kcal/mol. This indicates that, without an external electric field, the driving force for the pyrolysis reaction primarily originates from the thermal energy of the system itself, with no significant influence from external conditions. Under the 150 GHz frequency, the curve exhibits the highest fluctuations in potential energy. Over a certain time range, the potential energy increases and remains at a relatively high level for an extended period. This suggests that the alternating electric field at 150 GHz has the most pronounced promoting effect on the system. The resonance effect between the frequency and the system may optimize energy transfer, thereby accelerating molecular reactions and facilitating kerogen decomposition. At this frequency, the higher potential energy of the system indicates that more energy is absorbed, promoting the progress of the pyrolysis reaction. At other frequencies, the potential energy changes exhibit some degree of fluctuation, but compared to 150 GHz, the promoting effects of these frequencies are weaker. Although certain frequencies (200 GHz) show significant fluctuations, the overall rate of potential energy increase is slower, and the system rarely maintains a high energy level. In particular, at 50 GHz and 100 GHz, the potential energy fluctuates frequently but does not sustain a high value, suggesting that the electric fields at these frequencies may cause energy overload or fail to achieve resonance with the system, limiting their depolymerization effect on kerogen. At higher frequencies (200 GHz, 250 GHz, 300 GHz), although the potential energy fluctuates considerably, it does not remain at a high level. This may be due to energy overload or a mismatch with the resonance effects of the system, leading to a weakened promoting effect of the electric field. Consequently, despite the fluctuations in potential energy, the overall promoting effect is less pronounced compared to that at 150 GHz. Based on the potential energy curves, it can be inferred that the electric field at 150 GHz significantly increases the potential energy of the system, likely through resonance effects that make molecular bonds more prone to breaking, thereby accelerating the pyrolysis process of kerogen.

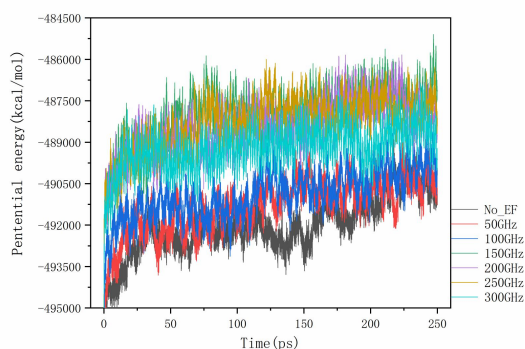


Figure. 5 Variation curve for the potential energy of the reaction system at different electric field frequencies.

#### 4. Conclusion

The application of external electric fields, especially at resonant frequencies like 150 GHz, enhances the pyrolysis of kerogen by promoting molecular breakdown and altering product distributions. The electric field's role in reducing bond dissociation energy barriers through resonance effects accelerates hydrocarbon generation while minimizing undesired coke formation. This study provides a theoretical foundation for utilizing electric fields to optimize kerogen pyrolysis, contributing to more efficient energy extraction from unconventional resources like shale oil and gas. Further investigations are required to refine the optimal frequency and fully understand the interaction mechanisms between electric fields and kerogen's molecular structure.

#### References

- [1] Wang X, Han X, You Y, Jiang X. Molecular characterization of Dachengzi oil shale kerogen by multidimensional solid-state nuclear magnetic resonance spectroscopy. *Fuel*, 2021, 303: 121215.
- [2] Han W, Luo X, Tao S, Lin S, Liu J, Yang Y. Activation energy and organic matter structure characteristics of shale kerogen and their significance for the in-situ conversion process of shale oil. *Fuel*, 2024, 307: 131823
- [3] Shi K, Chen J, Pang X, Jiang F, Hui S, Zhang S, Pang H, Wang Y, Chen D, Yang X, Li B, Pu T. Average molecular structure model of shale kerogen: Experimental characterization, structural reconstruction, and pyrolysis analysis. *Fuel*, 2024, 355: 129474.
- [4] He L, Ma Y, Yue C, Li S, Tang X. Microwave pyrolysis of oil shale for high-quality oil and gas production. *Journal of Thermal Analysis and Calorimetry*, 2022, 147: 9083-9093.
- [5] Su C, Liu Y, Yang Y, Gao T, Qi T, Wang Y. Evolution of aromatic structure and nanopores in shale kerogen by using in-situ HRTEM and in-situ FT-IR experiment. *Fuel*, 2024, 359: 130479.
- [6] Liu J, Yang Y, Sun S, Yao J, Kou J. Flow behaviors of shale oil in kerogen slit by molecular dynamics simulation. *Chemical Engineering Journal*, 2022, 434: 134682.
- [7] Zhang X, Guo W, Pan J, Zhu C, Deng S. In-situ pyrolysis of oil shale in pressured semi-closed system: Insights into products characteristics and pyrolysis mechanism. *Energy*, 2024, 286: 129608.
- [8] Zhang Y, Jiang Y, Li G, Duan X, Chen B. Reaction mechanism and kinetics of kerogen dehydrogenation and cyclization investigated by density functional theory. *Fuel*, 2024, 371: 131972.
- [9] Ma G, Chen J, Yue C, Ma Y, Gong L, Wang Y, Jiang F, Pang H, Niu X. Reaction molecular dynamics simulation of kerogen hydrogenation catalysis in marine deep shale. *Fuel*, 2025, 380: 133245.
- [10] Wang Y, Han X, Jiang X. A surrogate shale oil model based on a multi-objective fusion adaptive optimization considering its pyrolysis characteristics. *Energy*, 2024, 291: 130273.

- [11] Zhang Y, Wu W, Chen B. Exploring the influence of external electric fields on the catalytic pyrolysis of oil shale kerogen molecules. *International Communications in Heat and Mass Transfer*, 2024, 158: 107838.
- [12] Savostin G, Tikhonova M, Kalmykov A, Volkov D, Kostyshina M, Vidshcheva O, Makhnutina M, Kotochkova Y, Grigorenko T Proskurnin M. Effectof of Temperature on kerogen Transformation and Hydrocarbon Generation in Bazhenov Formation (Western Siberia, Russia) Rocks During Hydrous Pyrolysis. *Energies*, 2025, 18: 23.
- [13] Katti D, Thapa K, Katti K. Modeling molecular interactions of sodium montmorillonite clay with 3D kerogen models. *Fuel*, 2017, 199: 641-652.
- [14] Yang Q, Guo M, Guo W. Effects of Associated Minerals on the Co-Current Oxidizing Pyrolysis of Oil Shale in a Low-Temperature Stage. *ACS Omega*, 2021 6:23988-23997.
- [15] Zhang X, Cai F, Jin S, Liu H, Fang R, Wu Y. The effect of electric field on the pyrolysis of transformer insulation oil-paper based on molecular dynamics. *AIP Advances*, 2023, 13: 164038.
- [16] Zhang Y, Wu W, Chen B. Exp;roing the influence of external electric fields on the catalytic pyrolysis of oil shale kerogen molecules. *International Communications in Heat and Mass Transfer*, 2024, 158: 107838.
- [17] Van Duin A, Dasgupta S, Lorant F, Goddard W. ReaxFF: a reactive force field for hydrocarbons. *Journal de PhysiqueChem A*, 2001, 105: 9396-409.
- [18] Chen J, Martinez T. QTPIE: Charge transfer with polarization current equalization. A fluctuating charge model with correct asymptotics. *Chemical Physics Letters*, 2007, 438: 315-320.
- [19] Koski J, Moore S, Clay R, O'Hearn K, Aktulga H, Wilson M, Rackers J, D.Lane J, Modine N. Water in an External Electric Field: Comparing Charge Distribution Methods Using ReaxFF Simulations. *J. Chem. Theory Comput*, 2022, 18: 580-594.
- [20] Rappe A, Goddard W. Charge Equillbration for Molecular Dynamics Simulations. *J. Phys. Chem*, 1991, 95: 3358-3363.
- [21] Zhang Z, Chai J, Zhang H, Guo L, Zhan J. Structural model of LongKou oil shale kerogen and the evolution process under steam pyrolysis based on ReaxFF molecular dynamic simulation. *Energy Sources, Part A: Recovery, Utilization, and Environmental Effects*, 2019, 41:115-128.
- [22] Wood M, van Duin A, Strachan A. Coupled thermal and electromagnetic induced decomposition in the molecular explosive  $\alpha$ HMX; A reactive molecular dynamics study. *Journal de PhysiqueChem A* 2014, 118: 885-95.